

TOF- $B\rho$ Mass Measurements of Very Exotic Nuclides for Astrophysical Calculations at the NSCL

M Matoš^{1,2}, A Estrade^{1,2,3}, M Amthor^{1,2,3}, A Aprahamian^{2,4},
D Bazin¹, A Becerril^{1,2,3}, T Elliot^{1,2,3}, D Galaviz^{1,2}, A Gade^{1,3},
S Gupta⁷, G Lorusso^{1,2,3}, F Montes^{1,2}, J Pereira^{1,2}, M Portillo¹,
A M Rogers^{1,2,3}, H Schatz^{1,2,3}, D Shapira⁵, E Smith^{2,6}, A Stolz¹
and M Wallace⁷

¹ National Superconducting Cyclotron Laboratory, Michigan State University, East Lansing, MI, USA

² Joint Institute of Nuclear Astrophysics, Michigan State University, East Lansing, MI, USA

³ Department of Physics and Astronomy, Michigan State University, East Lansing, MI, USA

⁴ Institute of Structure and Nuclear Astrophysics, Department of Physics, University of Notre Dame, South Bend, IN, USA

⁵ Oak Ridge National Laboratory, Oak Ridge, TN, USA

⁶ Department of Physics, The Ohio State University, Columbus, OH, USA

⁷ Los Alamos National Laboratory, Los Alamos, NM, USA

E-mail: matos@nscl.msu.edu

Abstract. Atomic masses play a crucial role in many nuclear astrophysics calculations. The lack of experimental values for relevant exotic nuclides triggered a rapid development of new mass measurement devices around the world. The Time-of-Flight (TOF) mass measurements offer a complementary technique to the most precise one, Penning trap measurements [1], the latter being limited by the rate and half-lives of the ions of interest. The NSCL facility provides a well-suited infrastructure for TOF mass measurements of very exotic nuclei. At this facility, we have recently implemented a TOF- $B\rho$ technique and performed mass measurements of neutron-rich nuclides in the Fe region, important for r-process calculations and for calculations of processes occurring in the crust of accreting neutron stars.

PACS numbers: 21.10.Dr, 26.50.+x, 26.60.+c, 29.27.Eg

1. Introduction

With a minimum rate requirement of the order of 0.01 particles per second and a measurement time shorter than 1 μ s, the TOF mass measurements offer a complementary technique to the most precise Penning trap measurements. An entire region of the chart of nuclides can be covered in just one experimental run, producing important data related to astrophysical calculations, tests of mass models, and other nuclear physics applications.

2. Principle of the TOF Mass Measurement Technique

Time-of-Flight mass measurements are based on a precise measurement of the time it takes a charged particle to travel between two points within a magnetic optics system with a magnetic rigidity $B\rho$. The mass of the ion is determined from the equation

$$\frac{m}{q} = \frac{B\rho}{v} = B\rho \frac{t}{L}, \quad (1)$$

where t is the time-of-flight of a particle with mass-to-charge ratio m/q and velocity v within the path length L . In the relativistic case the expression can be written as

$$\frac{m_0}{q} = B\rho \left(\frac{1}{v^2} - \frac{1}{c^2} \right)^{1/2} = B\rho \left(\frac{t^2}{L^2} - \frac{1}{c^2} \right)^{1/2}, \quad (2)$$

where c is the speed of light.

In reality, precise measurements of the path length and absolute measurements of magnetic rigidity are very difficult. Nevertheless, as the path length and the magnetic rigidity can be considered to be constant for a fixed configuration of the system, the direct relation between the time-of-flight and the mass-to-charge ratio can be found using the nuclides with well known mass values.

A typical beam line with a momentum acceptance of several percent does not fulfil the condition of constant $B\rho$ required for a high precision mass measurement. To overcome this problem, two solutions are adapted at existing TOF mass measurement facilities. A measurement of relative magnetic rigidity by a position measurement at a dispersive plane of the magnetic optics system is used at the SPEG spectrometer at GANIL [2] and at the NSCL TOF- $B\rho$ facility (discussed in this paper). These measurements have to address the Z dependence due to energy losses in a position sensitive detector. The other possibility, applied by TOFI at LANL [3] and IMS at GSI [4], is the use of isochronous mode in magnetic optics. In this case, the ions with higher velocities travel on the longer trajectories in such a way that ions with the same mass-to-charge ratios have the same time-of-flight values independently from their energies. This can be achieved for a non-relativistic case if

$$\frac{L}{B\rho} = \text{constant} \quad (3)$$

for the full acceptance of the beam line. For relativistic cases a term dependent on a mass-to-charge ratio starts to play an important role;

$$L \left[\left(\frac{1}{B\rho} \right)^2 + \left(\frac{1}{cm_0/q} \right)^2 \right]^{1/2} = \text{constant} \quad (4)$$

and the isochronicity is limited to nuclides within a small range of mass-to-charge ratios. This problem can be alleviated by an improved time-of-flight resolution for non-isochronous particles with decreased magnetic rigidity acceptance [5]. In this case, the statistical uncertainty does not have to suffer from the reduced rate as it is compensated by a better resolution, except for the region of the best isochronicity, where the resolution is not improved with smaller acceptance.

Measurements of the magnetic rigidity were recently reported at GSI for the IMS technique [6]. At the future GSI facility a pair of time-of-flight detectors allowing a velocity measurement has been proposed [7].

All the mentioned techniques are one-turn time-of-flight facilities except for the IMS, which uses a storage ring for multiple TOF measurements. This leads to a significantly better resolution and is important for resolving isomeric contaminants in the TOF spectra.

3. TOF- $B\rho$ Mass Measurement Method at the NSCL

At the NSCL a fast radioactive beam is produced in the A1900 fragment separator [8]. The 58 m long time-of-flight line starts at the A1900 extended focal plane and ends at the focal plane of the S800 spectrograph [9], as shown in Figure 1. Fast scintillator

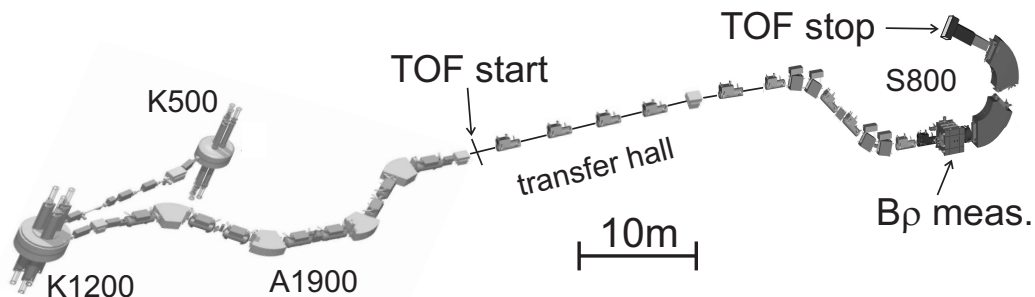


Figure 1. An overview of the facility. The primary relativistic beam is accelerated in the coupled cyclotrons K500-K1200. Radioactive ions are produced by fragmentation and separated in the A1900 fragment separator, where the TOF measurements start. The magnetic rigidity measurements are performed in front of the S800 spectrograph operated with dispersion matched optics. The TOF stop detector is placed at the S800 focal plane together with an ion chamber for energy loss measurement and CRDC detectors for particle tracking.

detectors provide the timing resolution of $\sigma=30$ ps. The relative magnetic rigidity is measured at the momentum dispersive plane by position-sensitive micro-channel plate detectors [10] with a position resolution of $\sigma=0.3$ mm. For more details refer to [11].

We also tested the operation of the magnetic optics system in an isochronous mode. A GICO calculation [12] was performed to find an isochronous magnetic optics setting. At the beginning of the experimental run, the isochronous mode was successfully achieved with a TOF resolution of $\sigma = 130$ ps, an improvement over the standard optics with $\sigma = 200$ ps as shown in Figure 2. However, for the TOF corrected with the measured magnetic rigidity a resolution of $\sigma = 80$ ps is achieved in the standard dispersion-matched optics mode. We therefore decided to use the TOF- $B\rho$ technique with standard optics.

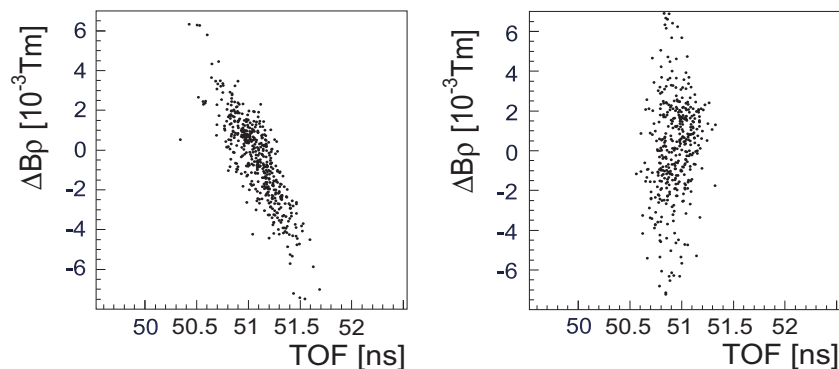


Figure 2. Measured TOF values of ^{79}Ga particles compared with their magnetic rigidities for standard (left panel) and isochronous (right panel) magnetic optics. Projected onto the TOF axis the TOF resolution is $\sigma = 200$ ps and $\sigma = 130$ ps respectively. In the case of standard optics the resolution corrected for the magnetic rigidity is $\sigma = 80$ ps.

4. Mass Measurement of Neutron-Rich ^{86}Kr Fragmentation Products

In the first TOF- $B\rho$ mass measurement at the NSCL a radioactive ion beam in the region of ^{68}Fe was produced by fragmentation of a relativistic 100 MeV/u ^{86}Kr primary beam on a solid Be target. Production targets with thicknesses of 46 mg/cm² and 94 mg/cm² were alternately used to populate a wide region of the chart of the nuclides in the secondary beam without the need for any change in the experimental settings.

The relative mass resolution of 2×10^{-4} obtained in the experiment allowed the relative statistical uncertainties to be $(1-3) \times 10^{-6}$. The systematic errors of the order of $(2-3) \times 10^{-6}$ in the preliminary analysis are expected to be reduced in the final results. Figure 3 shows the relative experimental uncertainties of mass measurements versus isobaric distance from stability (for details see [13]). The results from this work are compared with other mass measurement techniques. The presented technique has access

to more exotic nuclides with the NSCL radioactive beam facility and is competitive with SPEG mass measurements.

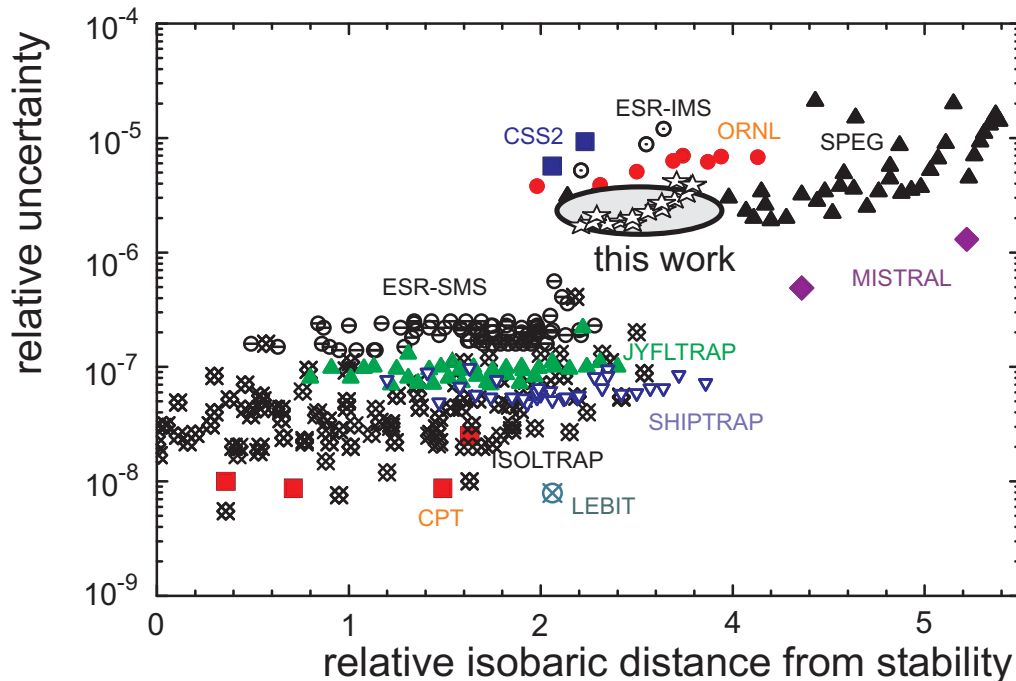


Figure 3. Relative experimental uncertainty of mass measurement results versus isobaric distance from stability for each nuclide obtained from [13] for comparison with our recent results. The results from this work are shown with open star symbols.

5. Application to Nuclear Astrophysics

5.1. Astrophysical *R*-Process Seed Nuclei

One of the leading candidates for the location of the *r*-process is the high entropy ejecta of Type II supernovae [14, 15]. In this scenario neutrinos not only revive the explosion via heating after the initial shock wave stalls due to the in-falling material of outer layers, but also drive the material neutron-rich with the hardening of the $\bar{\nu}_e$ spectra relative to the ν_e spectra at later times.

As this neutron rich material initially consisting of neutrons, protons and α -particles expands adiabatically and cools, heavy particles are formed by a combination of charged-particle reactions (proton and α -captures) and neutron captures. As the temperature decreases, charged-particle reactions freeze-out and a subsequent neutron capture process proceeds if there are enough neutrons remaining.

The resulting abundances, when the charge-particle freeze-out occurs, serve as seeds for the subsequent neutron capture process [16, 17]. The abundances are sensitive to neutron separation energies not only when neutron captures take over but also to determine the initial seed composition. Mass values in the required region of nuclides

are partially covered by the experiment discussed in this paper. Figure 4 shows the abundance composition at the moment of charge-particle freeze-out for a case with the entropy of $100 k_B \text{ baryon}^{-1}$ and the initial proton-to-nucleon ratio $Y_e = 0.45$.

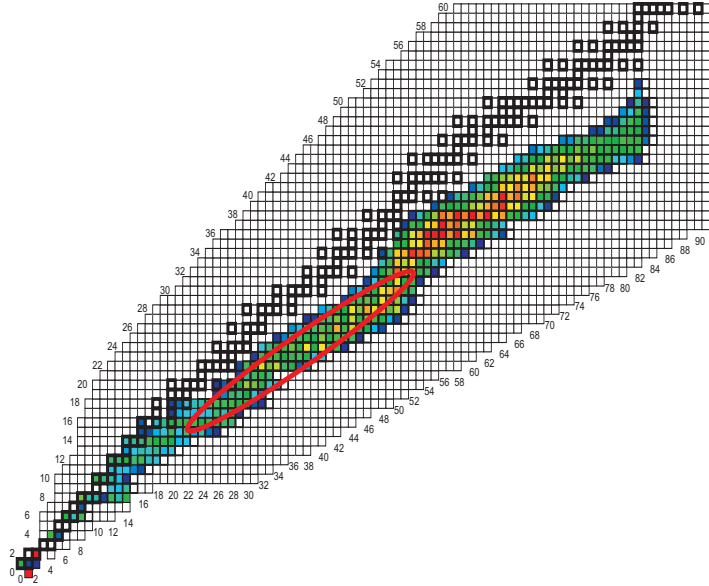


Figure 4. Abundance composition at the moment of charge-particle freeze-out in the high entropy ejecta of a Type II supernova simulation for entropy $100 k_B \text{ baryon}^{-1}$ and proton-to-nucleon ratio $Y_e = 0.45$. The reaction network is described in [17]. The area, covered in this experiment, is marked.

5.2. Heating of the Accreting Neutron Star Crust and Superburst

Processes occurring after accretion of matter onto neutron stars in binary systems have been related to observables in X-ray binaries. The ashes of the rp-process sink deeper into the crust and the electron chemical potential μ_e rises with the increasing density.

A calculation, seeding on a single beta-stable even-even rp-process nuclide, was performed in [18, 19]. Two processes were the primary deep crustal heating sources; pycnonuclear fusion at $\rho > 10^{12} \text{ g/cm}^2$, and two-stage electron-capture at densities $\rho > 10^{11} \text{ g/cm}^2$ that includes cold n-emission to maintain mechanical equilibrium within a Wigner-Seitz cell beyond cold neutron drip density.

New X-ray observations have led to the discovery of superbursts that are roughly 10^3 times more energetic compared to Type I X-ray bursts [20]. The thermally unstable ignition of ^{12}C at $\rho > 10^9 \text{ g/cm}^2$ was a proposed scenario for superbursts [21, 22], although the heat production in the deep crust would not be sufficient to explain observed superburst recurrence timescales of less than 10 years [23, 24].

The recent calculations of crustal heating using a realistic mix of rp-ashes [25] and including electron capture into excited states followed by a radiative deexcitation predict increased heating and therefore shallower superburst ignition and lower recurrence times between 2–3 years.

The results are very sensitive to the nuclear physics of neutron-rich nuclei up to $A=106$. In particular masses are needed for electron capture thresholds, heating rates from excited state captures, and the separation energies playing a crucial role in neutron reaction rates. New mass measurements in this region, including the experiment discussed in this paper, are important for the calculation to replace the FRDM mass model values [26] that were used.

6. Conclusions

The mass values in the region covered by this work are crucial for astrophysical calculations such as the investigation of the thermal balance in the crust of accreting neutron stars or the calculation of r-process seeding nuclei.

Experimental masses for neutron-rich nuclides have often been shown to be unreliable [27, 28] and new mass measurements are required.

The technique presented in this work is expected to enable the measurements of nuclides far from stability with relative uncertainties of the order of 2×10^{-6} . This method is now established at the NSCL coupled-cyclotron facility and will be used to measure masses of numerous very exotic nuclides.

References

- [1] Blaum K 2006 *Phys. Reports* **425** 1
- [2] Mittag W 1997 *Annu. Rev. Nucl. Part. Sci.* **47** 27
- [3] Wouters J M et al 1985 *Nucl. Instrum. Methods* **240** 77
- [4] Hausmann M et al. 2000 *Nucl. Instrum. Methods* **A446** 569
- [5] Matoš M 2004 Ph.D. Thesis, Justus Liebig Universität Giessen, Germany
<http://geb.uni-giessen.de/geb/volltexte/2004/1582>
- [6] Chen L et al 2006 GSI Scientific Report 2005 141
- [7] Matoš M 2006 *AIP Conf. Proc.* **819** 164
- [8] Stolz A et al 2005 *Nucl. Instrum. Methods* **B241** 858
- [9] Bazin D et al 2000 *Nucl. Instrum. Methods* **B204** 629
- [10] Shapira D et al 2000 *Nucl. Instrum. Methods* **A454** 409
- [11] Estrade A, Matoš M et al 2006 *Proc. of Int. Symp. Nuclei in the Cosmos IX, PoS(NIC-IX)* 092
- [12] Wollnik H et al 1988 *AIP Conf. Proc.* **177** 74
- [13] Lunney D 2006 *Proc. of Int. Symp. Nuclei in the Cosmos IX, PoS(NIC-IX)* 010
- [14] Cowan J J, Thielemann F-K and Truran J W 1991 *Phys. Rep.* **208** 267
- [15] Woosley S E and Hoffman R D 1992 *Astrophys. J.* **395** 202
- [16] Freiburghaus C et al 1999 *Astrophys. J.* **516** 381
- [17] Farouqi K et al 2007 to be published
- [18] Haensel P and Zdunik J L 1990 *Astron. Astrophys.*, **227** 431
- [19] Haensel P and Zdunik J L 2003 *Astron. Astrophys.*, **404** L33
- [20] Kuulkers E 2003 *Nucl. Phys. B. Proc. Suppl.* **132** 466
- [21] Schatz H, Bildsten L and Cumming A 2003 *Astrophys. J.* **583** L87
- [22] Cumming A and Bildsten L 2001 *Astrophys. J.*, **559** L127
- [23] Wijnands R 2001 *Astrophys. J.* **554** L59
- [24] Kuulkers E et al 2004 *AIP Conf. Proc.* **714** 257
- [25] Gupta S et al 2006 submitted to the *Astrophys. J.* (Preprint astro-ph/0609828)

- [26] Möller P et al 1995 *At. Data Nucl. Data Tables* **59** 185
- [27] Matoš M et al 2005 *Proc. Int. Symp. on Exotic Nuclei 2004 (Peterhof, Russia)* ed Yu E Penionzhkevich and E A Cherepanov (Singapore: World Scientific) p 90
- [28] Matoš M et al 2005 *Proc. Int. Symp. on Exotic Nuclei 2004 (Peterhof, Russia)* ed Yu E Penionzhkevich and E A Cherepanov (Singapore: World Scientific) p 96